

LA-UR-10-01605

Approved for public release;
distribution is unlimited.

<i>Title:</i>	The Contour Method Cutting Assumption: Error Minimization and Correction
<i>Author(s):</i>	Michael B. Prime, W-13 Alan L. Kastengren, Argonne National Lab
<i>Intended for:</i>	Prime, M. B., and Kastengren, A. L., 2011, "The Contour Method Cutting Assumption: Error Minimization and Correction," Experimental and Applied Mechanics, Volume 6, T. Proulx, ed., Springer New York, pp. 233-250. DOI: 10.1007/978-1-4419-9792-0_40.



Los Alamos National Laboratory, an affirmative action/equal opportunity employer, is operated by the Los Alamos National Security, LLC for the National Nuclear Security Administration of the U.S. Department of Energy under contract DE-AC52-06NA25396. By acceptance of this article, the publisher recognizes that the U.S. Government retains a nonexclusive, royalty-free license to publish or reproduce the published form of this contribution, or to allow others to do so, for U.S. Government purposes. Los Alamos National Laboratory requests that the publisher identify this article as work performed under the auspices of the U.S. Department of Energy. Los Alamos National Laboratory strongly supports academic freedom and a researcher's right to publish; as an institution, however, the Laboratory does not endorse the viewpoint of a publication or guarantee its technical correctness.

The Contour Method Cutting Assumption: Error Minimization and Correction

Michael B. Prime (prime@lanl.gov), Alan L. Kastengren*
Los Alamos National Laboratory, Los Alamos, NM 87545

* Now at the Energy Systems Division, Argonne National Laboratory

ABSTRACT

The recently developed contour method can measure 2-D, cross-sectional residual-stress map. A part is cut in two using a precise and low-stress cutting technique such as electric discharge machining. The contours of the new surfaces created by the cut, which will not be flat if residual stresses are relaxed by the cutting, are then measured and used to calculate the original residual stresses.

The precise nature of the assumption about the cut is presented theoretically and is evaluated experimentally. Simply assuming a flat cut is overly restrictive and misleading. The critical assumption is that the width of the cut, when measured in the original, undeformed configuration of the body is constant. Stresses at the cut tip during cutting cause the material to deform, which causes errors. The effect of such cutting errors on the measured stresses is presented. The important parameters are quantified. Experimental procedures for minimizing these errors are presented. An iterative finite element procedure to correct for the errors is also presented. The correction procedure is demonstrated on experimental data from a steel beam that was plastically bent to put in a known profile of residual stresses.

INTRODUCTION

Residual stresses play a significant role in many material failure processes like fatigue, fracture, stress corrosion cracking, buckling and distortion [1]. Residual stresses are the stresses present in a part free from any external load, and they are generated by virtually any manufacturing process. Because of their important contribution to failure and their almost universal presence, knowledge of residual stress is crucial for prediction of the life of any engineering structure. However, the prediction of residual stresses is a very complex problem. In fact, the development of residual stress generally involves nonlinear material behavior, phase transformation, coupled mechanical and thermal problems and also heterogeneous mechanical properties. So, the ability to accurately quantify residual stresses through measurement is an important engineering tool.

Recently, a new method for measuring residual stress, the contour method [2-4], has been introduced. In the contour method, a part is carefully cut in two along a flat plane causing the residual stress normal to the cut plane to relax. The contour of each of the opposing surfaces created by the cut is then measured. The deviation of the surface contours from planarity is assumed to be caused by elastic relaxation of residual stresses and is therefore used to calculate the original residual stresses. One of the unique strengths of this method is that it provides a full cross-sectional map of the residual stress component normal to the cross section. The contour method is useful for studying various manufacturing processes such as laser peening [5-10], friction welding [6,7,11-13] and fusion welding [14-21]. Some of the applications are quite unique such as mapping stresses in a railroad rail [22], in the region of an individual laser peening pulse [23], and under an impact crater [24].

The only common methods that can measure similar two-dimensional (2-D) stress maps have significant limitations. The neutron diffraction method is nondestructive but sensitive to micro-structural changes [25], time consuming, and limited in maximum specimen size, about 50 mm, and minimum spatial resolution, about 1mm. Sectioning methods [26] are experimentally cumbersome, analytically complex, error prone, and have limited spatial resolution, about 1 cm. A limitation of the original contour method is that only one residual stress component is determined. Recent developments have extended the contour method to the measurement of multiple stress components [27-30].

In an overly simplistic view, one might think that the contour method requires the assumption of a perfectly flat cut. Such an assumption is overly restrictive. In this paper, the actual assumptions about the cut are developed. Several potential error sources are shown to be removed by standard data processing. Other errors are explored in more detail numerically to establish procedure to minimize the errors. An experimental demonstration is given with a correction for errors arising because of the cut.

THEORY

This section reviews previously published theory for the contour method in order to allow for later detailed discussion of the assumption about the cut.

The contour method [2] shown in Figure 1 is based on a variation of Bueckner's superposition principle [31].

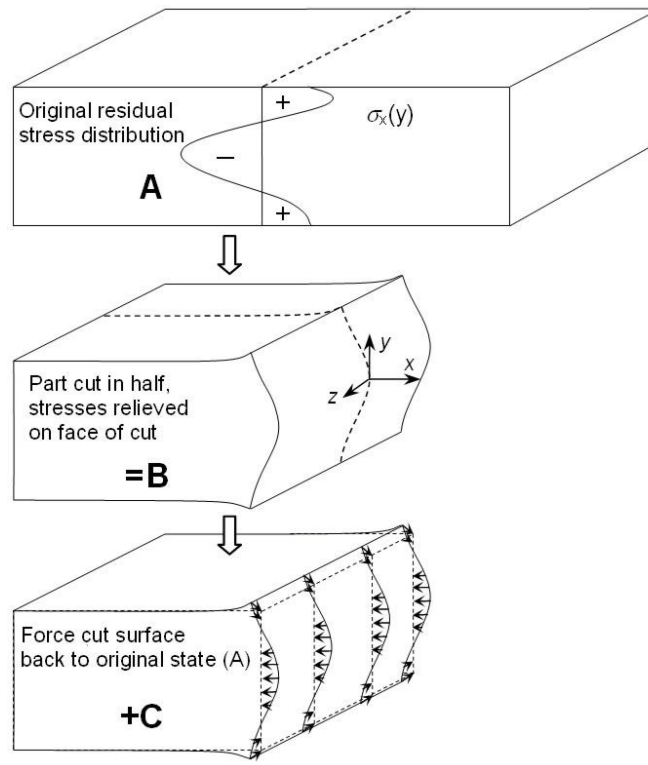


Figure 1 Superposition principle to calculate residual stresses from surface contour measured after cutting the part in two [28].

In **A**, the part is in the undisturbed state and contains the residual stress to be determined. In **B**, the part has been cut in two and has deformed as residual stresses were released by the cut. For clarity, only one of the halves is shown. In **C**, the free surface created by the cut is forced back to its original flat shape. Assuming elasticity, superimposing the partially relaxed stress state in **B** with the change in stress from **C** would give the original residual stress throughout the part:

$$\sigma^{(A)} = \sigma^{(B)} + \sigma^{(C)} \quad (1)$$

where σ without subscripts refers to the entire stress tensor.

This superposition principle assumes elastic relaxation of the material and that the cutting process does not introduce stress that could affect the measured contour. With proper application of this principle it is possible to determine the residual stress over the plane of the cut. Experimentally, the contour of the free surface is measured after the cut and analytically the surface of a stress-free model is forced back to its original flat

configuration by applying the opposite of the measured contour as boundary conditions. Because the stresses in **B** are unknown, one cannot obtain the original stress throughout the body. However, the normal and shear stresses on the free surface in **B** must be zero (σ_x , τ_{xy} and τ_{xz}). Therefore, **C** by itself will give the correct stresses along the plane of the cut:

$$\begin{aligned}\sigma_x^{(A)} &= \sigma_x^{(C)} \\ \tau_{xy}^{(A)} &= \tau_{xy}^{(C)} \\ \tau_{xz}^{(A)} &= \tau_{xz}^{(C)}\end{aligned}\tag{2}$$

The measured surface contour has an arbitrary reference plane, resulting in three arbitrary rigid body motions in defining the surface. These three arbitrary motions are uniquely determined by the need for the stress distribution over the cross section to satisfy three global equilibrium conditions: force in the x-direction and moments about the y and z axes. It is not necessary to explicitly enforce these constraints. In a finite element calculation, appropriate boundary conditions are applied to the cut plane, including three extra constraints to prevent rigid body motions. The remainder of the body is unconstrained. In the static equilibrium step used to solve for stress, the free end of the body will automatically translate and rotate such that the equilibrium conditions are fulfilled.

A small convenience is taken in the data analysis. Modeling the deformed shape of the part for **C** in Figure 1 would be tedious. Instead, the surface is flat in the finite element model, and then the part is deformed into the shape opposite of the measured contour. Because the deformations are quite small, the same answer is obtained but with less effort.

CUTTING ASSUMPTION

From a theoretical point of view, the relevant assumption for the superposition principle in Figure 1 is that the material points on the cut surface are returned in **C** to their original configuration. Experimental limitations results in two broad types of departures from that assumption. The first departure is that the surface contour measurement only gives information about the normal (x) displacement. So the material points are not returned to their original configuration in the transverse directions. The second departure is that in order for the measured surface contour to accurately return the material points to their original locations in the x-direction, those material points must have come from a common plane in the original configuration (**A**).

A transformation of this theoretical assumption into more practical assumptions can accommodate some of these issues without sacrificing any accuracy. This naturally leads to considering symmetric errors separate from antisymmetric errors, as explained in the following.

Anti-Symmetric Errors

The issues with both transverse displacements and anti-symmetric errors can be examined by considering the case of shear stresses [2]. The top of Figure 2 shows a beam that was cut in half on a plane that had both normal and shear stresses. The two halves have different contours. The equivalent surface traction components for released stresses are given by $T_x = -\sigma_x n_x$, $T_y = -\tau_{xy} n_x$, where n is the surface normal vector. By a Poisson effect, the T_y from the released shear stress has an effect on the contour. As shown in Figure 2 in reference [2], the tractions for releasing σ_x are symmetric about the cut plane, but the tractions for releasing τ_{xy} are anti-symmetric. Hence, the contours in Figure 2 can be decomposed into the symmetric portion caused by normal stress and the anti-symmetric portion caused by shear stress.

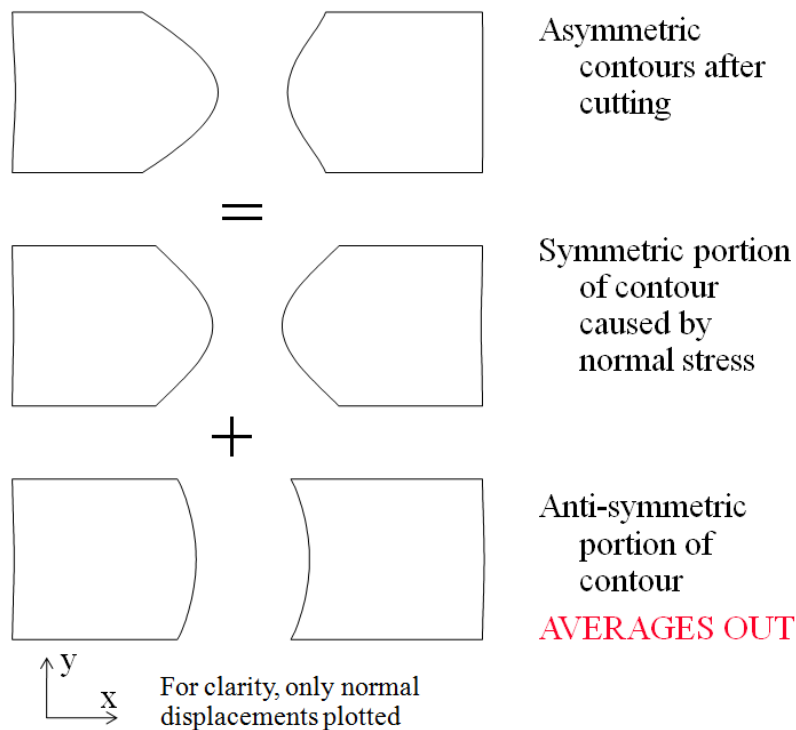


Figure 2. Asymmetric contours can be separated into the symmetric portion and the anti-symmetric portion, which averages away. Shown for the example of shear stresses.

The effect of shear stresses, and indeed all anti-symmetric errors, are removed by averaging the contours on the two halves.

The lack of information on transverse displacements also does not cause errors. In the analysis, the surface is forced back (step **C** in Figure 1) to the original flat configuration only in the x -direction, based on the average contour. The shear stresses (τ_{xy} and τ_{xz}) are constrained to zero in the solution. This stress-free constraint is automatically enforced in most implicit, structural, finite-element analyses if the transverse displacements are left unconstrained. Even if residual shear stresses were present on the cut plane, averaging the contours measured on the two halves of part still leads to the correct determination of the normal stress σ_x [2]. Even when there are no shear stresses, there are also transverse displacements from a Poisson-type effect when normal stresses are relaxed. Because there was no shear stress, there is no traction associated with those displacements. Therefore, the solution that constrains the shear stresses to zero on the cut surface, as described above, is still correct.

Averaging the contours on the two halves to remove anti-symmetric errors requires another assumption. The portion of the contour caused by the normal stress must be symmetric, which requires that the stiffness be the same on the two sides of the cut. For homogeneous materials, this assumption is certainly satisfied when a symmetric part is cut precisely in half. In practice, the part only needs to be symmetric about the cut within the region where the stress release has a significant effect. The length of this region is about 1.5 times the Saint Venant's characteristic distance. The characteristic distance is often as the part thickness, but is more conservatively taken as the maximum cross-sectional dimension unless specific information about the stress variation is known [12].

Figure 3 shows another example of an anti-symmetric error that averages away. If cut path is crooked in space, the resulting surface contours are anti-symmetric.

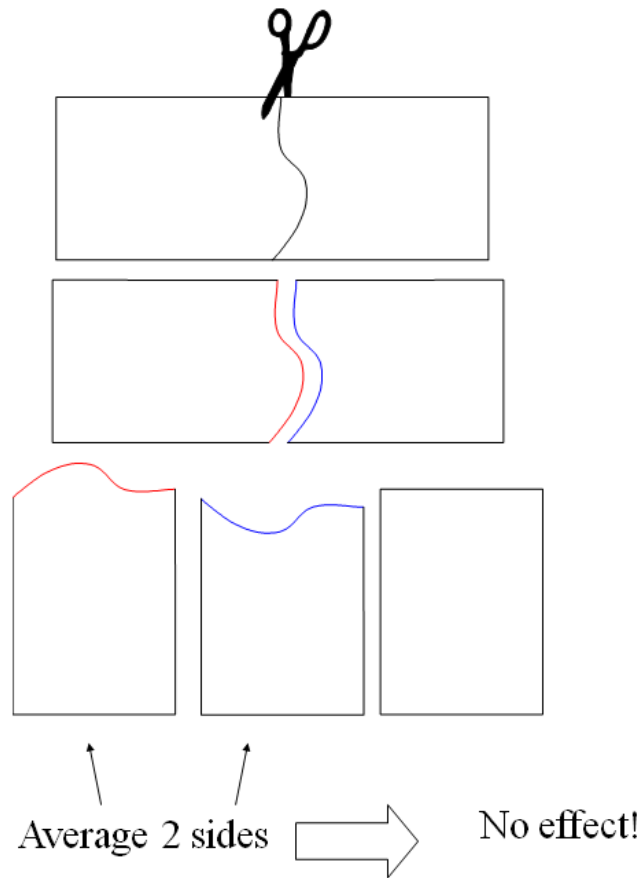


Figure 3. The effect of a crooked cut goes away when the two surfaces contours are averaged.

Figure 4 shows another anti-symmetric effect that in principle averages away, but that should be minimized anyway. This time the cut path is straight in space, but the part is moving as the stresses relax. In Figure 4, the movement occurs because the part is not clamped symmetrically. An experimental example later in this paper shows that the effect can be quite large. Averaging two very different contours can introduce some uncertainty, so both sides of the cut should be clamped to minimize such movement. It will be shown later that other errors are also reduced by good clamping.

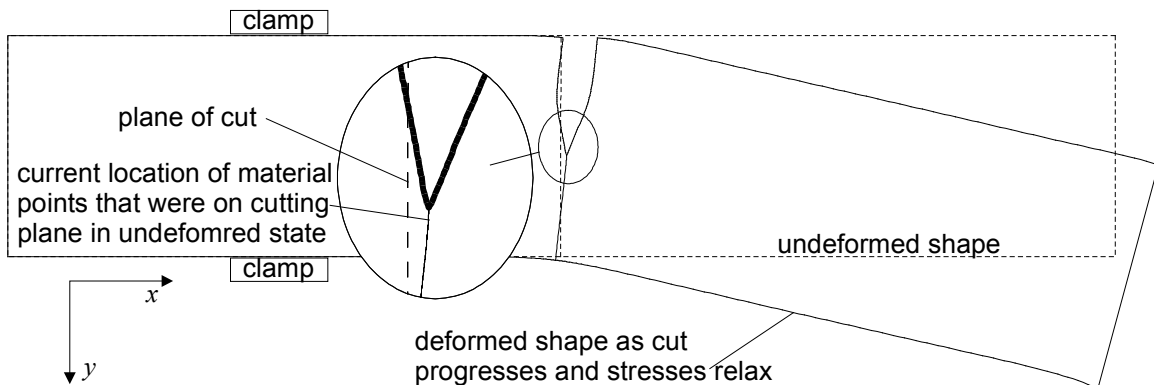


Figure 4. Movement of the cut plane as stresses relax during cutting. In this example, this is caused by asymmetric clamping.

Symmetric Errors

There are other errors that cause symmetric effects that do not average way. Before discussing those, realize that some cutting errors depend on how the cut is made. So far, the only method that has been successfully applied for the contour method is wire Electric Discharge Machining (EDM). Thus, this discussion focuses on EDM cutting.

Several of the symmetric error sources are relatively straightforward:

- Local cutting irregularities, such as wire breakage or overburning at some foreign particle. These are usually small length scale (order of wire diameter) and are removed by the data smoothing process or manually from the raw data
- Change in width of cut. This can occur in heterogeneous materials since the EDM cut width varies for different materials. Sometimes a change in the part thickness (wire direction) can also cause this.
- Wire vibration causing a “bowed” cut [2]. This can usually be avoided by using good settings on the wire EDM.
- Stresses induced by the cutting process can cause errors. Such errors have been studied for wire EDM cutting for use with incremental slitting (crack compliance) [32]. Such effects are generally negligible if “skim cut” or “finish cut” EDM settings are used. Those are low power settings that give higher accuracy and a better surface finish.

The symmetric error sources listed above do not depend on stress magnitude, which leads to a straightforward approach to the issue. A test cut in stress free material would have no contour caused by stresses but would show these errors. Any such error could then be corrected for by subtracting the error off of the measured contour. Most good practitioners make such a test cut standard practice. The simplest way to achieve a nearly stress free test cut is to use the actual test part. After surface contours are measured, one can cut a thin layer off of one of the cut surfaces. The relevant stress components are zero on the free surface and very small if the test cut occurs only a small distance from the original cut surface. The surface contour is measured on the new surface of the larger piece.

Some of those assumptions, primarily the constant cut width, may be less accurate near the edges of the cut surface. For example, the EDM cut width may flare out a little bit at the top and bottom of the cut. Contour results can therefore be quite uncertain near the edges of the cut and should not be generally be reported in that region. With special care, good results have been achieved very close to the edges [4,23].

The contour cut also cannot re-cut previously cut surfaces. This is one of the main reasons that EDM is used for the contour method. In principle, EDM might slightly recut the surface when cutting into a compressive stress. In practice, as sketched in Figure 5, constraint at the cut tip minimizes the amount the cut surfaces can pinch in close behind the wire.

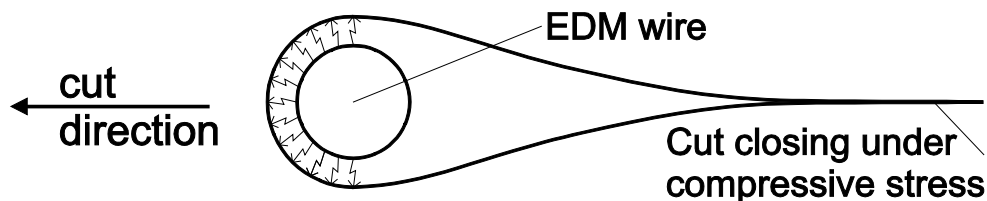


Figure 5. Even cutting into compressive stress, constraint limits the amount the cut surfaces can pinch in close behind the wire.

Most of the rest of this paper will concern a particular symmetric error that can cause significant bias in the contour method results if it is not dealt with. This error, called the “bulge” error, is illustrated in Figure 6. The cutting process makes a cut of constant width w in the laboratory reference frame. As the cutting proceeds, stresses relax and the material at the tip of the cut deforms. The material at the cut tip that was originally w wide has stretched. However, the physical cut will still be only w wide, which means that the width of material removed has been reduced when measured relative to the original state of the body. Since the fundamental assumption is that step **C** of Figure 1 returns the material points to their original configuration, this causes an error that will not

be averaged away. The effect is obviously dependent on the stress state at the cut tip relative of the original stress state. That change in stress can be minimized by securely clamping the part. Also, this effect is a result of the finite width of the cut; a zero-width crack causes only effects that average away, as shown in Figure 4.

Considering anti-symmetric effects that average away as well as the bulge and other asymmetric errors, the fundamental assumption about the cut can be more compactly stated. The cutting process is assumed to remove a constant width of material when measured relative to the state of the body prior to any cutting.

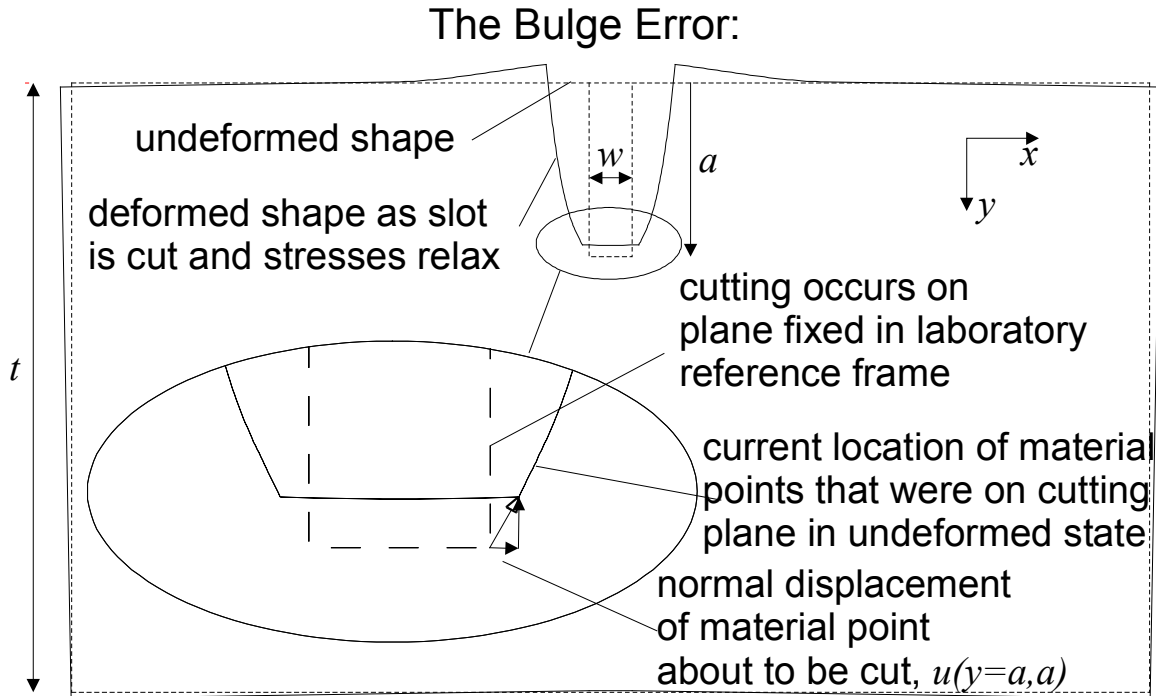


Figure 6. The “bulge” error. As cutting proceeds, the material at the tip of the cut deforms from stress relief. This changes the width of the cut relative to the original state of the body and causes errors.

Cut tip plasticity can also cause symmetric errors. Such errors violate the assumption that stress relaxation is elastic, rather than assumptions about the cut, but they cause very similar effects. Like the bulge error, this effect also depends on the stress state at the cut tip. Thus, any efforts to minimize the bulge error should also reduce plasticity errors. An FEM study showed that plasticity errors were generally small when clamping during cutting was secure [33]. Another study that looked at experimental results showed some significant errors that were explained, using FEM, by plasticity effects [34]. However, those experimental errors might have been a combination of both bulge and plasticity errors.

Summary of Assumptions

- The cutting process does not recut surfaces that have already been cut.
- The stiffness of the part is symmetric with respect to the cut within the regions where stresses are relaxed by the cut
- The cut removes a finite width of material when measured relative to the state of the body prior to any cutting.
- There is no plasticity at the cut tip

The ideal cut would be zero width, introduce no stresses, and allow no plasticity at the tip of the cut.

FINITE ELEMENT STUDY

Finite Element Models

The bulge error was estimated using two-dimensional ABAQUS [35] finite element simulations of sequentially cutting a slot into a beam, similar to Figure 6. A known field of residual stresses was used as an initial condition for the model using a user-defined subroutine. The cutting process was then simulated by sequentially removing elements. After each step, the displacement of appropriate material points originally on the cut plane were recorded to estimate errors in the planar cut assumption. Finally, residual stresses were calculated using the principle of Figure 1 but including the errors, and the difference between the calculated residual stresses and the known residual stresses were analyzed.

Several assumptions were used for the simulations. Isotropic, linear elastic material behavior is assumed throughout the analysis. It is also assumed that the cut is perfectly planar in space; hence, the deviations come only from deformation of the material. For meshing convenience, a square slot bottom was used. Since an EDM cut has a round bottom, this assumption may introduce errors. Dimensions of the beam were normalized to a beam thickness, t , of one unit. A total beam length of four units was chosen in order to minimize any effects from the free ends. Plane stress deformation was assumed.

Legendre polynomials were chosen for the residual stresses because Legendre polynomials of order two and greater automatically satisfy force and moment equilibrium over the beam cross section. For each simulation, the appropriate Legendre polynomial was used to initialize $\sigma_x(y)$ in the region of the cut. The other two stress components, σ_y and τ_{xy} , were initialized to zero in the region of the cut. The stresses elsewhere in the beam were specified such that local equilibrium and the stress-free boundary conditions were satisfied everywhere. The residual stress distributions were all normalized to a peak value of unity.

The choice of the elastic modulus E has no effect on the final stress values calculated from the displacements, since it proportionally affects both the error magnitude and the actual contour. Nonetheless, an E of 1000 was used rather in order to give reasonably scaled displacements; the σ_{\max}/E ratio of 0.001 is consistent with typical residual stress magnitudes in metals. Since E has no effect on the final stresses calculated, plane strain can be simulated by replacing E with $E/(1-\nu^2)$; plane stress and plane strain will give the same results if the analysis is consistent.

The deviations from a planar cut assumption were estimated by considering the displacement of the material point where cutting is about to occur. Referring to Figure 6, the material point at the bottom corner of the slot is the next to be cut. The material point that was originally on the plane where cutting is occurring has displaced. In the actual cutting process, the wire will cut this point flush with the original cut plane. Therefore, the deviation from the flat cut assumption is given by the displacement of this material point normal to the cut plane, in the x direction. The y -displacement is not important.

A Lagrangian coordinate system is used to track the deformations. The displacements $u(x,y,a)$ refers to the x -direction displacement after the cut is at depth a of the material point that was at the coordinate (x,y) in the original configuration of the system. Because the only displacement that is relevant for this simulation is the displacement of points at the fixed value of x for the cut plane, the displacement is reported just as $u(y,a)$. The final contour of the cut surface is given by the displacements after the cut and is designated by $u(y,final)$. The results of the sequential cutting simulation were used as input to a subsequent analysis to calculate the effect of the cutting deviation on the residual stress measurements of the contour method. The final contour of the cut surface from the simulation was combined with the cutting error to give the displacement boundary conditions used to calculate the residual stress per the third part of Figure 1:

$$u(y) = -(u(y, final) - u(y = a, a)), \quad (1)$$

where the initial negative sign appears because calculating the original residual stresses requires applying the opposite of the measured contour.

This stress calculation makes two additional assumptions. The small displacements of the material on the cut plane were not accounted for in the material removed for the simulation. The simulation removed elements with edges that were originally on the cut plane but were no longer on the cut plane at the time of removal. Because the displacements are small, the difference has a negligible effect on the results of the stress calculations. An

exact simulation of the material removal would require adaptive remeshing or some other process, and such extra effort is not justified by the small changes that would result.

Simulation Results: General Features of the Contour Method and the Errors

There are several interesting features in almost all of these simulations. Typical deflection and cutting error profiles are shown in Figure 7 for a simple clamping arrangement: on the top and bottom surfaces of the beam at one thickness away from the cut, symmetric on both sides of the cut. The slot width is 0.01. The quadratic Legendre polynomial stress is used. The bulge error has a shape that is not the same as the stress profile. Rather, the bulge error is approximately proportional to the stress intensity factor, $K_{I,RS}$, at the cut tip from the accumulated effect of releasing residual stress. Combining the bulge error with the theoretical contour gives the contour including the error. The general shape of the contour with cutting error closely parallels that of the deflection without cutting error. The deflection profile has a slightly smaller peak when the cutting error is included. It also shows a phase shift compared to the profile without cutting error, with the peak values shifted closer to the beginning of the cut. Near the end of the cut, the deflection error rises sharply, causing a large difference between the two profiles.

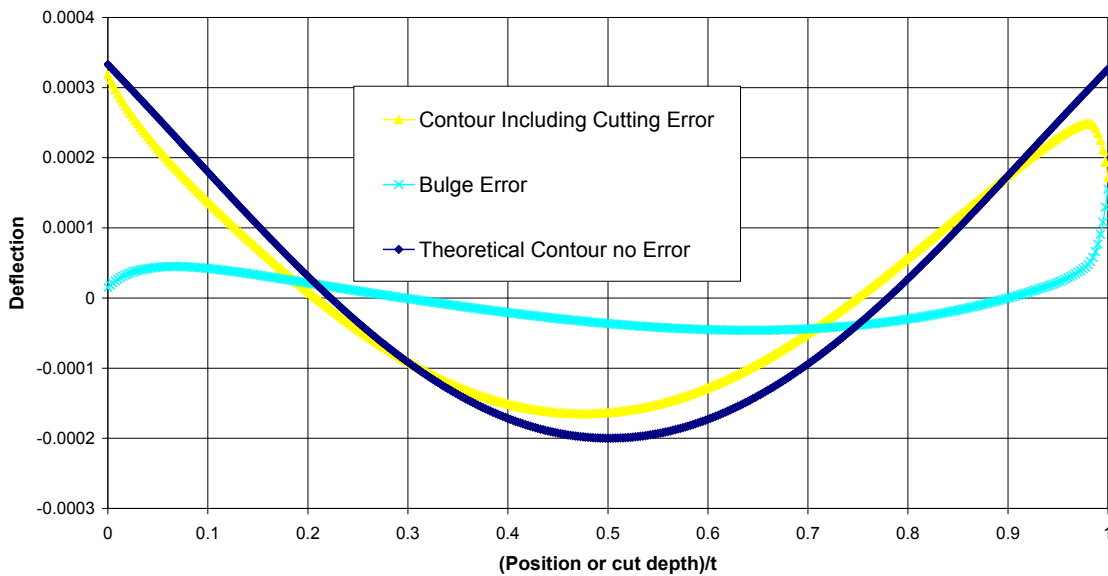


Figure 7. Bulge error for a FEM simulation of a quadratic stress profile.

The stress profiles in Figure 8 show most of the same features as the deflection profiles. The stress error is high near the beginning of the cut and very high near the end of the cut. This matches with the experiences in the actual measurement process, where the edges often show erratic behavior. However, the effect seems to be exaggerated in these simulations. More work is needed to improve the fidelity of the simulations at the beginning and end of the cut. Near the middle of the cut, the stress error is quite reasonable and seems to follow a smooth curve. Again, it does not seem to be simply related to the initial stress distribution, though a great deal of the error seems to be a phase shift between the profiles with and without cutting error. The peak compressive stress is slightly reduced in magnitude.

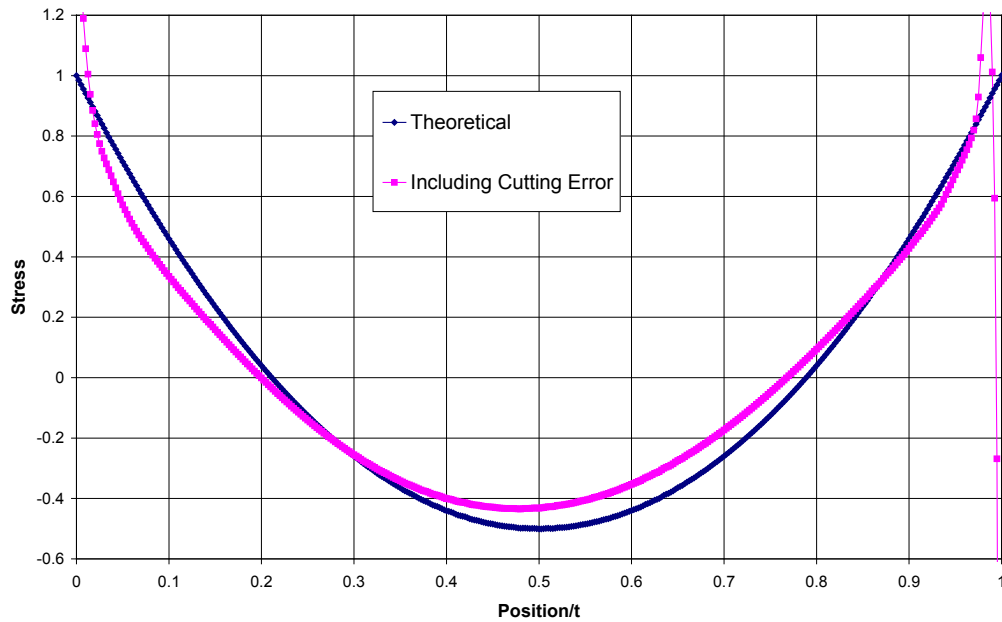


Figure 8. Stresses calculated from the contours of Figure 7 showing the stress error caused by the bulge error.

Effect of Clamping

A variety of clamping arrangements were simulated by constraining various nodes in the FEM model from moving. Because of the difficulty of achieving experimental clamping similar to the perfect constraint, only qualitative conclusions are presented:

- A significant benefit is achieved by going from clamping on one side of the cut to clamping both sides of the cut.
- In the simulations, a significant benefit is achieved by clamping the material all along the cut rather than just at the top and bottom surfaces. However, this is difficult to achieve experimentally.
- Modest but diminishing benefits are achieved by moving the clamping closer to the cut.

Effect of Slot Width

Another simulation examined the effect of slot width on the error. A zig-zag stresses profile typical of beam bending was used as the initial stress. The beam was clamped symmetrically on both sides of the cut. The FEM mesh was adjusted to give different slot widths. Figure 9 shows curves of bulge error as a function of cut depth relative to the beam thickness. The final contour (without error) is also plotted to illustrate the scale of the errors. The bulge error gets larger for larger cut width. The peak magnitude of the bulge error was extracted from each curve in Figure 9, normalized by the peak-to-valley magnitude of the contour, and plotted versus slot width in Figure 10. The peak error increases with slot width, with the slope being greater for narrow slots. A typical experimental slot width, taken from the beam tests to be discussed in the next section, is indicated in order to place the errors in proper context.

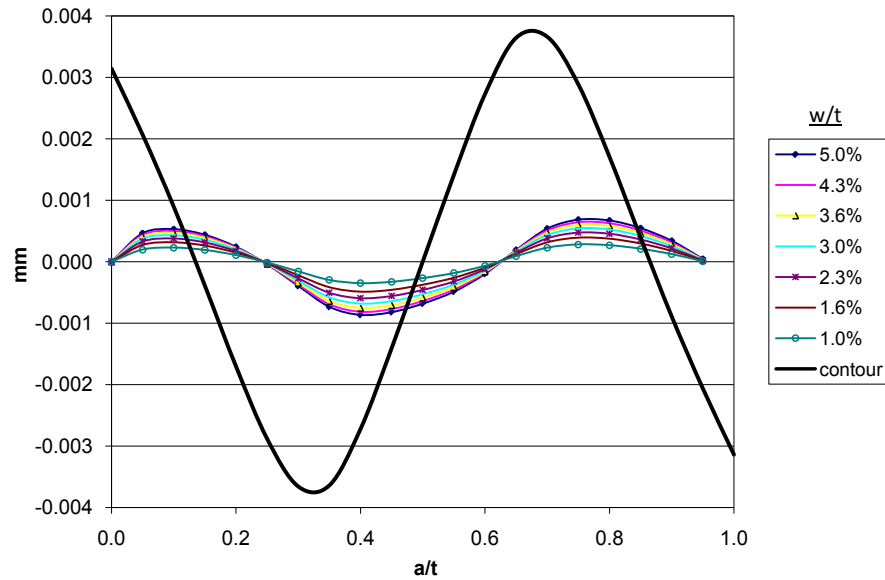


Figure 9. Bulge error as a function of cut depth for different slot widths relative to the beam thickness. The final contour (without error) is also plotted to illustrate the scale of the errors.

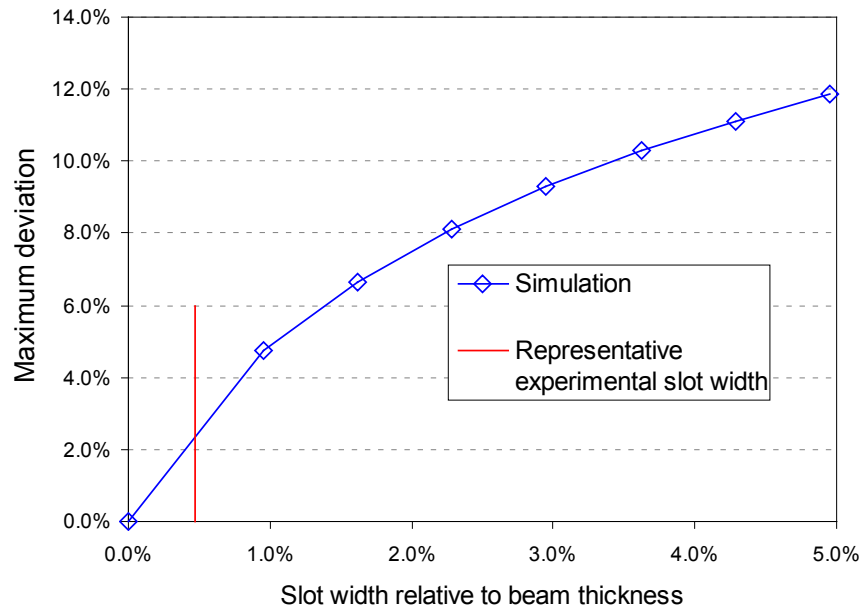


Figure 10. The peak values of bulge error from Figure 9 are normalized relative to the peak-to-peak amplitude of the measured contour and plotted versus slot width.

PROCEDURE FOR CORRECTING BULGE ERROR

The previous analysis, when applied to realistic slot widths, shows that the errors in the residual stress measurement are very reasonable, especially when compared to the errors in other residual stress measurement techniques. However, a method to correct these errors could improve the measurements by this technique.

An iterative finite-element analysis is proposed to correct the deflection error. The basic principle is to reverse the previous analysis technique. The experimentally measured or recorded profile is used to calculate residual stress. Since the errors in the contour method are relatively small, and the measurable deflection profile closely

parallels the theoretical profile, the calculated stress profile can be used as an initial guess for the theoretical profile. Then the FEM simulation described above is used to estimate the bulge error. The bulge error is used to correct the measured contour and then to calculate stresses now including an estimated bulge error. This process is then repeated until the stress converges.

EXPERIMENTAL

The bulge error and the iterative correction are examined on two bent beam specimens with known residual stress profiles. To prepare the specimen, strain gages were attached to the top and bottom of a stress-relieved stainless steel beam, 30.0mm deep. Residual stresses were induced in the beam by loading it into the plastic range using a four-point bend fixture. On removal of the load, the beam unloaded elastically, leaving permanent plastic deformations and substantial axial residual stresses. During this loading and unloading, the total load and corresponding strains were measured. The profile of the residual stresses was calculated from the measured strain data using the stress-strain curve identification method described by Mayville and Finnie [36]. More details on these specific beams are given elsewhere [2,37].

The first beam, beam A, was used as a known stress specimen for measurements using incremental slitting (crack compliance). As is standard with the slitting method [38], the beam was only clamped on one during the cutting as shown in Figure 11. The one sided clamping will make for a larger bulge error and different contours on the two halves of the beam. Before destructive measurement, the residual stresses in the beam were measured by neutron and x-ray diffraction, and within the associated uncertainty ranges, the results agreed with those of the stress-strain curve calculation [37,39]. A 200 μm diameter hard brass wire was used for the cutting. The cutting was done in 36 steps, at approximately 0.8mm intervals to a final depth of 29.26 mm, 97.5% of the beam depth. After cutting, the width of the cut was measured as 267 μm . Unfortunately, because the beam had not been cut all the way through, the remaining ligament was fractured by hand. That left the final 0.74 mm of the surface without a usable contour.

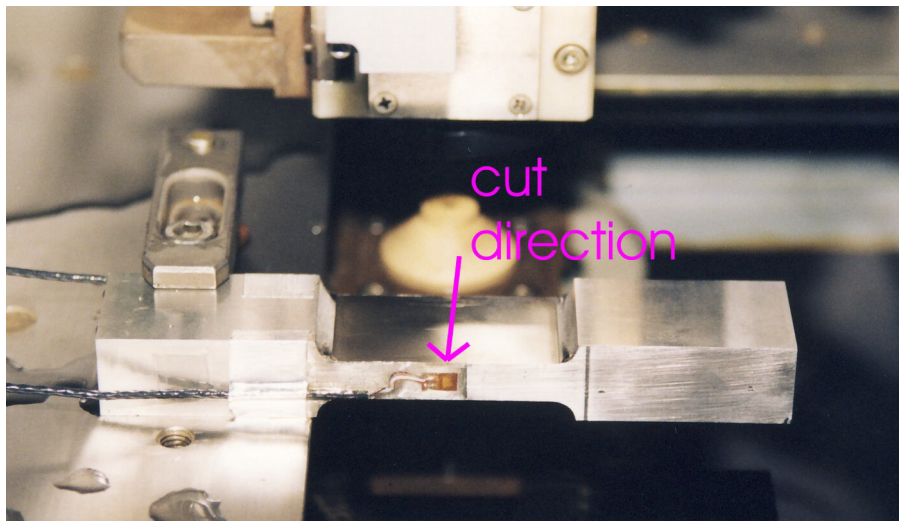


Figure 11. Beam A just prior to EDM cutting for the slitting method. The central section of the beam is 30 mm thick and 10 mm wide.

The second beam, beam B, was measured with the contour method [2]. As shown in Figure 12, it was clamped on both sides of the cut. This time the EDM cut used a 100 μm diameter zinc-coated brass wire and gave a cut width of 140 μm . The beam was cut all the way in half.

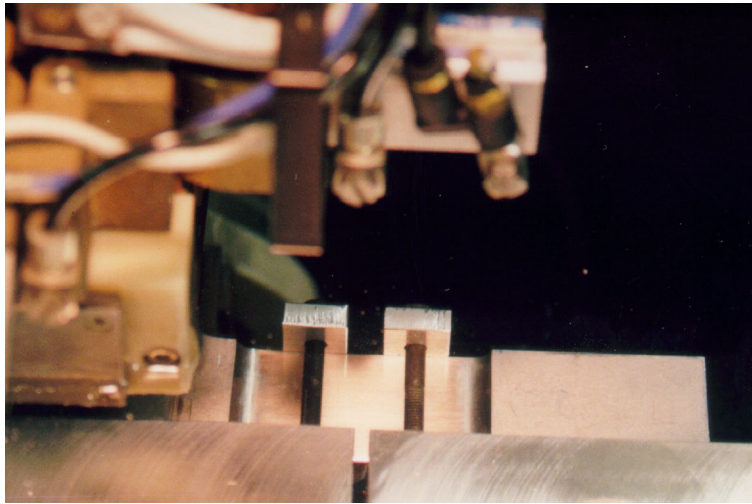


Figure 12. Beam B was clamped on both sides of the cut prior to EDM cutting.

Beam B

Beam B is examined first because it was cut under more ideal conditions: a narrow slot and clamped on both sides of the cut. The contours on the two halves of the beam were very similar, so the average was used for all subsequent calculations. By symmetry, only half of the beam was modeled (in 2D) with FEM. Displacement boundary conditions were applied on the top and bottom surfaces of the beam where the clamps from Figure 12 were located. Figure 13 shows the contours calculated with the iterative correction procedure. Because the correction is small, the correction has converged by the second iteration. Figure 14 shows the stress results compared with the stresses predicted in the bend test. The correction, while not large, has moved the contour results closer to the bend test prediction. Now the results generally agree within the uncertainty in the bend test prediction.

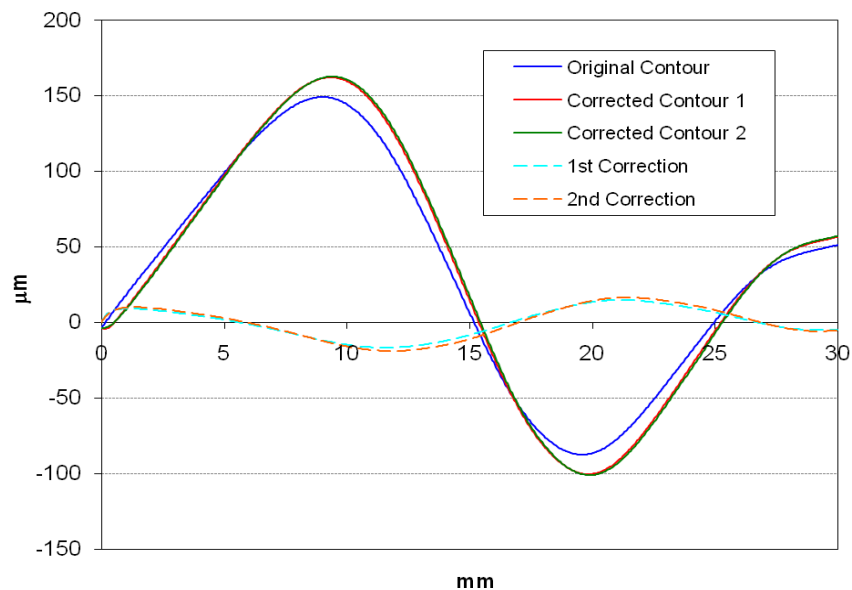


Figure 13. Iterative correction to measured contour on beam B.

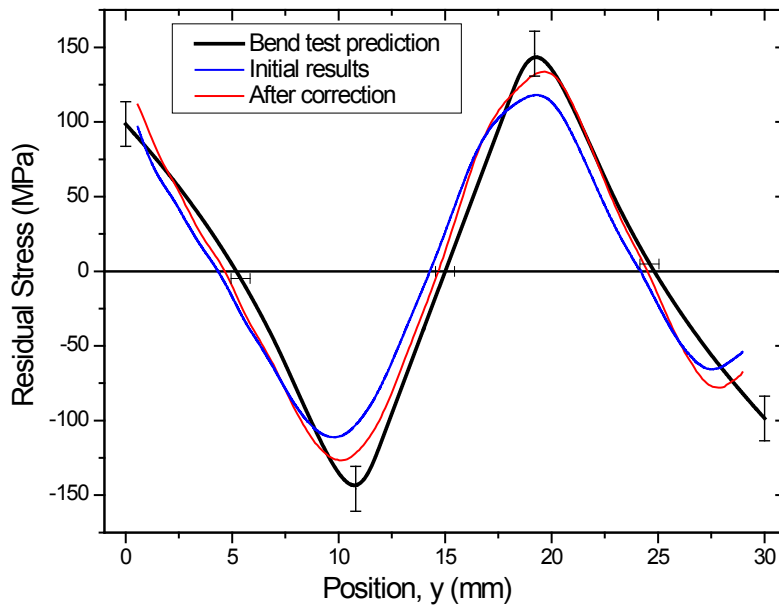


Figure 14. Contour method results before and after bulge correction compared with the prediction from the bend test.

Beam A

Because it was cut in such a non-ideal way for the contour method, with a wide slot and one sided clamping, beam A represents a challenging test for the iterative correction. Figure 15 shows the drastic difference between the contours measured on the two halves of the beam. Figure 16 shows results from beam A calculated using the average contour as well as using the contour from each half individually. The results are compared with bend test prediction and slitting and neutron diffraction measurements [39]. In spite of the large difference in the contours, the stresses calculated using the average contour do an impressive job of matching the bend test prediction and independent measurements.

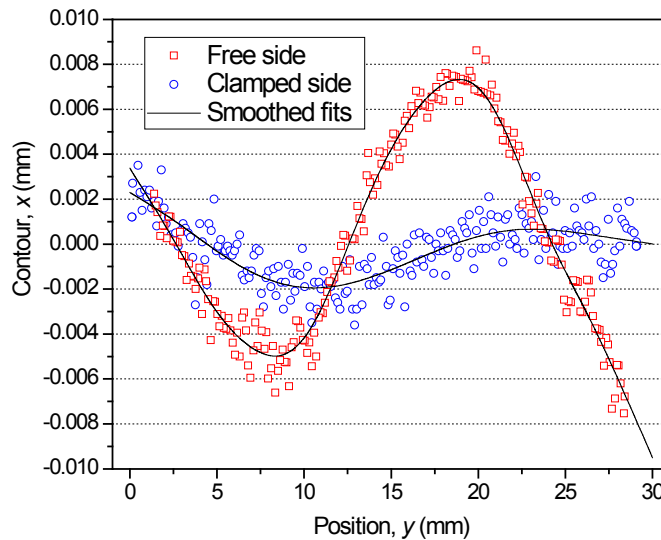


Figure 15. The surface contours measured on the two halves of beam A are very different.

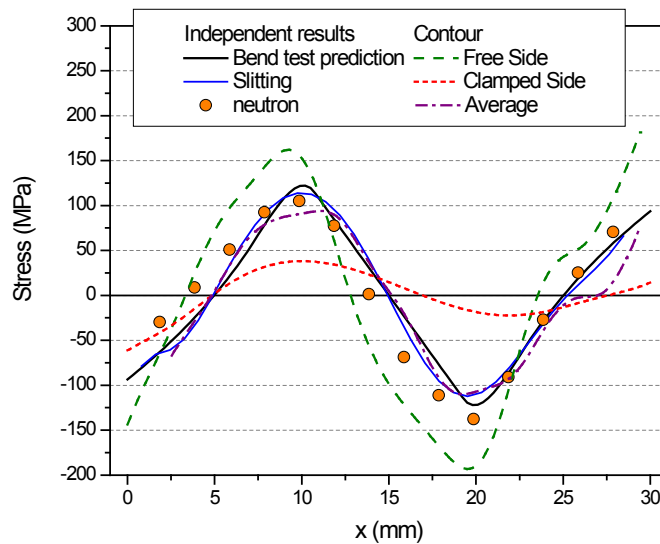


Figure 16. Stress results from beam A calculated using the average contour as well as using the contour from each half individually. Results compared with bend test prediction and slitting and neutron diffraction measurements.

A full 2D (no symmetry) FEM model was used to perform the iterative correction on the beam A results. Displacement boundary conditions were applied on the top and bottom surfaces of the beam where the clamps from Figure 11 were located. The contours had to be extrapolated to cover the final 0.74 mm of the surface that had been fractured off.

Because the contour on the free side of beam A over-predicted the stress magnitude, see Figure 16, the correction was also over-predicted, which led to a non-convergent solution. So for the first iteration only, half of the predicted correction was applied. Figure 17 shows that the correction was then reasonably stable and converged after several iterations. The average of the last two iterations compares quite well with the stresses predicted by the bend test.

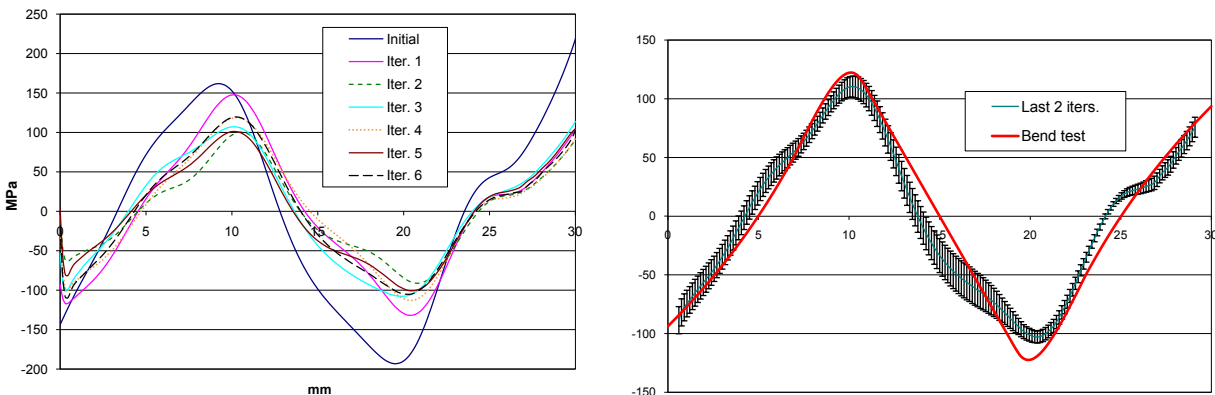


Figure 17. Iterative correction applied to the unclamped half of beam A.

Considering the starting point for the clamped half of beam A, a good result from the iterative correction was not expected. The results in Figure 15 and Figure 16 do not even have the correct shape. Figure 18 shows the iterative correction. Even though the results are poor at the ends of the beam, the central results slowly converge towards the expected results from the bend test analysis.

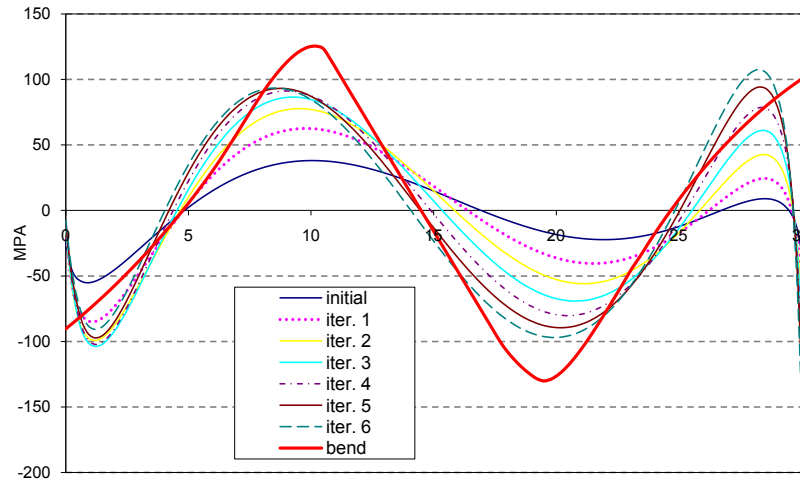


Figure 18. The iterative correction applied to the clamped half of beam A.

DISCUSSION

Both the bulge effect and plasticity errors (only briefly mentioned in this paper) are apparently dependent on the stress state at the cut tip, which can be characterized by the intensity factor, K_{IRS} , at the cut tip from the accumulated effect of releasing residual stress. Similar strategies could be used for both effects. More secure clamping, e.g., [20], would experimentally minimize the errors. Analytical corrections based on fracture mechanics analysis might be successful. Because of the dependence on K_{IRS} , such errors will depend on the direction of the cut.

Although the bulge error decreases for decreasing cut width, other errors might increase. Some difficulties getting good cuts with wire under 100 μm diameter have been observed.

The iterative correction procedure using FEM is promising. Some improvements need to be made on handling the beginning and end of the cut. The procedure is conceptually straightforward and was demonstrated in 2D. There is no conceptual difficulty in applying the procedure in 3D, but keep track of displacements at all the correct nodes for each cut depth would be tedious. A scripting procedure could simplify matters. Scripting interfaces are now available for many commercial finite element codes.

CONCLUSION

The assumptions about the cut for the contour method are

- The cutting process does not recut surfaces that have already been cut.
- The stiffness of the part is symmetric with respect to the cut within the regions where stresses are relaxed by the cut
- The cut removes a finite width of material when measured relative to the state of the body prior to any cutting.
- There is no plasticity at the cut tip

Deviations from these assumptions can cause errors:

- Cutting errors can be divided into errors that cause perturbations to the measured contours that are anti-symmetric with respect to the cut plane, and those that are symmetric. Anti-symmetric errors are removed by averaging the contours measured on the two halves of the part. Symmetric errors do not average away.
- The bulge error, a symmetric error, tends to cause stress profiles to show both a reduced peak stress magnitude and a spatial shift of the peaks
- The bulge error depends on the direction of the cut
- The bulge error is reduced the more securely material near the cut is clamped

- The bulge error decreases for decreasing slot width
- The bulge error can be modeled with FEM and an iterative correction is possible.
- Larger errors are expected at the beginning and end of the cut.

The ideal cut would be zero width, introduce no stresses, and allow no plasticity at the tip of the cut.

Some conclusions can be made about best practices for the contour method:

- The part should be clamped securely on both sides of the cut during cutting
- A stress-free test cut should be used as a control check on cutting assumptions. The test cut can be achieved after the contour measurement by cutting a thin slide off of the cut surface.
- Contour results are uncertain near the edges of the cut and should not be reported in that region unless special care is used to get better results there.

ACKNOWLEDGEMENTS

This work was performed at Los Alamos National Laboratory, operated by the Los Alamos National Security, LLC for the National Nuclear Security Administration of the U.S. Department of Energy under contract DE-AC52-06NA25396. By acceptance of this article, the publisher recognizes that the U.S. Government retains a nonexclusive, royalty-free license to publish or reproduce the published form of this contribution, or to allow others to do so, for U.S. Government purposes.

REFERENCES

- [1] Withers PJ (2007) Residual Stress and Its Role in Failure. Reports on Progress in Physics 70:2211-2264.
- [2] Prime MB (2001) Cross-Sectional Mapping of Residual Stresses by Measuring the Surface Contour after a Cut. Journal of Engineering Materials and Technology 123:162-168.
- [3] Prime MB, Sebring RJ, Edwards JM, Hughes DJ, Webster PJ (2004) Laser Surface-Contouring and Spline Data-Smoothing for Residual Stress Measurement. Experimental Mechanics 44:176-184.
- [4] Johnson G, (2008), "Residual Stress Measurements Using the Contour Method," Ph.D. Dissertation, University of Manchester.
- [5] DeWald AT, Rankin JE, Hill MR, Lee MJ, Chen HL (2004) Assessment of Tensile Residual Stress Mitigation in Alloy 22 Welds Due to Laser Peening. Journal of Engineering Materials and Technology 126:465-473.
- [6] Hatamleh O, Lyons J, Forman R (2007) Laser Peening and Shot Peening Effects on Fatigue Life and Surface Roughness of Friction Stir Welded 7075-T7351 Aluminum. Fatigue and Fracture of Engineering Material and Structures 30:115-130.
- [7] Hatamleh O (2008) Effects of Peening on Mechanical Properties in Friction Stir Welded 2195 Aluminum Alloy Joints. Materials Science and Engineering: A 492:168-176.
- [8] DeWald AT, Hill MR (2009) Eigenstrain Based Model for Prediction of Laser Peening Residual Stresses in Arbitrary 3D Bodies. Part 2: Model Verification. Journal of Strain Analysis for Engineering Design 44:13-27.
- [9] Liu KK, Hill MR (2009) The Effects of Laser Peening and Shot Peening on Fretting Fatigue in Ti-6Al-4V Coupons. Tribology International 42:1250-1262.
- [10] Hatamleh O, DeWald A (2009) An Investigation of the Peening Effects on the Residual Stresses in Friction Stir Welded 2195 and 7075 Aluminum Alloy Joints. Journal of Materials Processing Technology 209:4822-4829.
- [11] Woo W, Choo H, Prime MB, Feng Z, Clausen B (2008) Microstructure, Texture and Residual Stress in a Friction-Stir-Processed AZ31B Magnesium Alloy. Acta Mat. 56:1701-1711.
- [12] Prime MB, Gnaupel-Herold T, Baumann JA, Lederich RJ, Bowden DM, Sebring RJ (2006) Residual Stress Measurements in a Thick, Dissimilar Aluminum Alloy Friction Stir Weld. Acta Mat. 54:4013-4021.
- [13] Frankel P, Preuss M, Steuwer A, Withers PJ, Bray S (2009) Comparison of Residual Stresses in Ti6Al4v and Ti6Al2sn4zr2mo Linear Friction Welds. Materials Science and Technology 25:640-650.
- [14] Zhang Y, Pratihari S, Fitzpatrick ME, Edwards L (2005) Residual Stress Mapping in Welds Using the Contour Method. Materials Science Forum 490/491:294-299.
- [15] Edwards L, Smith M, Turski M, Fitzpatrick M, Bouchard P (2008) Advances in Residual Stress Modeling and Measurement for the Structural Integrity Assessment of Welded Thermal Power Plant. Advanced Materials Research 41-42:391-400.

- [16] Kartal M, Turski M, Johnson G, Fitzpatrick ME, Gungor S, Withers PJ, Edwards L (2006) Residual Stress Measurements in Single and Multi-Pass Groove Weld Specimens Using Neutron Diffraction and the Contour Method. *Materials Science Forum* 524/525:671-676.
- [17] Withers PJ, Turski M, Edwards L, Bouchard PJ, Buttler DJ (2008) Recent Advances in Residual Stress Measurement. *The International Journal of Pressure Vessels and Piping* 85:118-127.
- [18] Zhang Y, Ganguly S, Edwards L, Fitzpatrick ME (2004) Cross-Sectional Mapping of Residual Stresses in a VPPA Weld Using the Contour Method. *Acta Mat.* 52:5225-5232.
- [19] Thibault D, Bocher P, Thomas M (2009) Residual Stress and Microstructure in Welds of 13%Cr-4%Ni Martensitic Stainless Steel. *Journal of Materials Processing Technology* 209:2195-2202.
- [20] Hacini L, Van Lê N, Bocher P (2009) Evaluation of Residual Stresses Induced by Robotized Hammer Peening by the Contour Method. *Experimental Mechanics* 49:775-783.
- [21] Turski M, Edwards L (2009) Residual Stress Measurement of a 316L Stainless Steel Bead-on-Plate Specimen Utilising the Contour Method. *International Journal of Pressure Vessels and Piping* 86:126-131.
- [22] Kelleher J, Prime MB, Buttler D, Mummery PM, Webster PJ, Shackleton J, Withers PJ (2003) The Measurement of Residual Stress in Railway Rails by Diffraction and Other Methods. *Journal of Neutron Research* 11:187-193.
- [23] Evans A, Johnson G, King A, Withers PJ (2007) Characterization of Laser Peening Residual Stresses in Al 7075 by Synchrotron Diffraction and the Contour Method. *Journal of Neutron Research* 15:147-154.
- [24] Martineau RL, Prime MB, Duffey T (2004) Penetration of HSLA-100 Steel with Tungsten Carbide Spheres at Striking Velocities between 0.8 and 2.5 km/s. *International Journal of Impact Engineering* 30:505-520.
- [25] Holden TM, Suzuki H, Carr DG, Ripley MI, Clausen B (2006) Stress Measurements in Welds: Problem Areas. *Materials Science and Engineering A* 437:33-37.
- [26] Schajer GS (2001) "Residual Stresses: Measurement by Destructive Testing." *Encyclopedia of Materials: Science and Technology*, Elsevier, 8152-8158.
- [27] DeWald AT, Hill MR (2006) Multi-Axial Contour Method for Mapping Residual Stresses in Continuously Processed Bodies. *Experimental Mechanics* 46:473-490.
- [28] Pagliaro P, (2008), "Mapping Multiple Residual Stress Components Using the Contour Method and Superposition," Ph.D. Dissertation, Università degli Studi di Palermo, Palermo.
- [29] Pagliaro P, Prime MB, Swenson H, Zuccarello B (2010) Measuring Multiple Residual-Stress Components Using the Contour Method and Multiple Cuts. *Experimental Mechanics* 50:187-194.
- [30] Kartal ME, Liljedahl CDM, Gungor S, Edwards L, Fitzpatrick ME (2008) Determination of the Profile of the Complete Residual Stress Tensor in a VPPA Weld Using the Multi-Axial Contour Method. *Acta Mat.* 56:4417-4428.
- [31] Bueckner HF (1973) "Field Singularities and Related Integral Representations." *Mechanics of Fracture* G. C. Sih, ed., 239-314.
- [32] Cheng W, Finnie I, Gremaud M, Prime MB (1994) Measurement of near-Surface Residual-Stresses Using Electric-Discharge Wire Machining. *Journal of Engineering Materials and Technology-Transactions of the ASME* 116:1-7.
- [33] Shin SH (2005) FEM Analysis of Plasticity-Induced Error on Measurement of Welding Residual Stress by the Contour Method. *Journal of Mechanical Science and Technology* 19:1885-1890.
- [34] Dennis RJ, Bray, D.P., Leggatt, N.A., Turski, M. , (2008), "Assessment of the Influence of Plasticity and Constraint on Measured Residual Stresses Using the Contour Method." *2008 ASME Pressure Vessels and Piping Division Conference*, Chicago, IL, USA, PVP2008-61490.
- [35] Abaqus 6.9, ABAQUS, inc., Pawtucket, RI, USA, 2009.
- [36] Mayville R, Finnie I (1982) Uniaxial Stress-Strain Curves from a Bending Test. *Experimental Mechanics* 22:197-201.
- [37] Schajer GS, Prime MB (2006) Use of Inverse Solutions for Residual Stress Measurements. *Journal of Engineering Materials and Technology* 128:375-382.
- [38] Cheng W, Finnie I (2007) *Residual Stress Measurement and the Slitting Method*, Springer Science+Business Media, LLC, New York, NY, USA.
- [39] Prime MB, Rangaswamy P, Daymond MR, Abeln TG, 1998, "Several Methods Applied to Measuring Residual Stress in a Known Specimen." *Proc. 1998 SEM spring conference on experimental and applied mechanics*, 1-3 Jun 1998, Society for Experimental Mechanics, Inc., 497-499.